Equation of State of the Energy landscape of **SPC/E** Water

C. J. Roberts, P. G. Debenedetti, and F. H. Stillinger

Department of Chemical Engineering, Princeton University, Princeton,
New Jersey, 08544, Bell Laboratories, Lucent Technologies, Inc.,
Murray Hill, New Jersey 07974, and Princeton Materials Institute,
Princeton University, Princeton, New Jersey 08544

Equation of State of the Energy Landscape of SPC/E Water

C. J. Roberts,[†] **P. G. Debenedetti,**[*,†] **and F. H. Stillinger**[‡,§]

Department of Chemical Engineering, Princeton University, Princeton, New Jersey, 08544, Bell Laboratories, Lucent Technologies, Inc., Murray Hill, New Jersey 07974, and Princeton Materials Institute, Princeton University, Princeton, New Jersey 08544

Received: June 3, 1999; In Final Form: August 24, 1999

The contributions to the thermodynamics of liquid SPC/E water from its inherent structures have been determined over a broad range of temperature and density (220−500 K, 0.8− 1.25 g/cm³). Molecular dynamics simulations of shifted-force SPC/E water give a retracing locus of density maxima in the equilibrium liquid with a retracing point at ca. 275 K and -200 bar, showing that over a large range of temperature and pressure the inherent structures correspond to a liquid with negative thermal expansion. Both the pressure and potential energy in the inherent structures show a strong dependence on the temperature of the liquid from which the mechanically stable packings are generated. The potential energy of the inherent structures also shows a striking behavior at low temperatures, attaining lower energies than the ground states of pure crystalline forms. This contrasts with simple molecular liquids having no orientation-dependent interactions and suggests novel microscopic interpretations for a number of water's anomalous properties, such as the polyamorphic transition between its glassy phases, and a fragile-to-strong transition as the liquid is supercooled to its vitreous form.

I. Introduction

The multidimensional potential energy hypersurface, or energy landscape, provides valuable information on complex behavior in condensed-phase systems. Examples include protein folding,[1] dynamics of glass-forming liquids,[2] and the glass transition.[3] It has recently been shown that the manner in which a simple glass-forming liquid samples its underlying landscape as a function of temperature offers insight into its dynamic behavior.[2] Similarly, sampling in density provides information on mechanical properties such as tensile strength.[4]

Except for a brief reference to water,[4] the idea of relating static and dynamic properties to the manner in which an energy landscape is sampled in temperature (T), and is changed as a function of density (p), has so far been applied only to simple, monatomic liquids.[2,4,5] In this work we extend this idea to water, the classic example of a molecular liquid with strong, orientation-dependent interactions. These interactions result in a number of distinctive, anomalous properties at temperatures close to, and below, the equilibrium freezing point. Examples include a negative thermal expansion coefficient $(\alpha_p < 0)$,[6−9] strongly increasing isobaric heat capacity (c_p) and isothermal compressibility (κ_T) upon isobaric cooling,[8,10−12] and the existence of distinct glassy phases (polyamorphism).[8,13,14] Using molecular dynamics simulation, we investigate the manner in which the SPC/E model of water[15] samples its underlying landscape as a function of T, and the manner in which the landscape changes as a function of p.

To introduce the concept of the equation of state of an energy landscape, we begin by considering the multidimensional potential energy surface Φ, which is a function of $(3+n)N$

degrees of freedom. Here, *n* denotes the number of rotational, vibrational, and conformational degrees of freedom of each of the N molecules in the system. The term landscape is a useful intuitive description of the geometry of the Φ hypersurface in the $[(3+n)N+1]$ space of variables (i.e., the $(3+n)N$ **configu**rational degrees of freedom, plus Φ). Although it is impossible to visualize such a hypersurface, the intuitive three-dimensional connotations associated with the notion of a landscape (valleys, peaks, ridges) are helpful pictorial descriptors of local energy minima and the barriers separating them. These minima are mechanically stable arrangements of the N particles, and satisfy the condition

$$\nabla_\Omega \Phi = 0 \qquad (1)$$

where Ω is the vector whose $(3+n)N$ components are the molecular configurational coordinates. The potential energy minima are often called inherent structures.[16] In the thermodynamic limit, there is an exponential multiplicity of inherent structures:[17] the number of distinct inherent structures characterized by a potential energy per particle $\phi \pm d\phi/2$ is given by

$$\exp[N\sigma(\phi)]d\phi \quad (\sigma \geq 0) \qquad (2)$$

There is, in addition, a trivial combinatorial multiplicity of inherent structures which results from particle exhanges giving rise to N! equivalent structures for each of the $\exp(N\sigma)$ included in eq 2. Each inherent structure has a well-defined basin of attraction, which is the set of configurations that are mapped onto the given minimum by the steepest descent operation of eq 1. Turning now to the concept of the equation of state of the landscape, we begin by noting that in general the pressure and configurational energy of an equilibrium system can be written as

* Corresponding author. E-mail: pdebene@princeton.edu.
† Department of Chemical Engineering.
‡ Bell Laboratories.
§ Princeton Materials Institute.

Energy Landscape of SPC/E Water

J. Phys. Chem. B, Vol. 103, No. 46, 1999 **10259**

$$p = [\sum_{\alpha} \sum_{j(\alpha)} e^{-\beta E_j}]^{-1} \sum_{\alpha} \sum_{j(\alpha)} p_j e^{-\beta E_j} \qquad (3)$$

and

$$\Phi = [\sum_{\alpha} \sum_{j(\alpha)} e^{-\beta E_j}]^{-1} \sum_{\alpha} \sum_{j(\alpha)} \Phi_j e^{-\beta E_j} \qquad (4)$$

where α enumerates the inherent strucures (IS), j enumerates all the configurations in the equilibrated system belonging to the basin of attraction of the given inherent structure, p_j is the pressure (ideal plus virial) corresponding to a given configuration, Φ_j is the potential energy corresponding to a given configuration, and $\beta = 1/k_B T$, with k_B denoting Boltzmann's constant. Similarly, we define the corresponding IS quantities

$$p^{IS} = [\sum_{\alpha} \sum_{j(\alpha)} e^{-\beta E_j}]^{-1} \sum_{\alpha} p_\alpha^{IS} \sum_{j(\alpha)} e^{-\beta E_j} \qquad (5)$$

and

$$\Phi^{IS} = [\sum_{\alpha} \sum_{j(\alpha)} e^{-\beta E_j}]^{-1} \sum_{\alpha} \Phi_\alpha^{IS} \sum_{j(\alpha)} e^{-\beta E_j} \qquad (6)$$

where p_α^{IS} and Φ_α^{IS} are the virial pressure[5] and potential energy, respectively, of the IS to which all configurations in its basin of attraction map uniquely. By analogy with the familiar concept of an equation of state, we define $p^{IS}(\rho,T)$ to be the equation of state of the energy landscape. Thus, the functions $p^{IS}(\rho,T)$ and $\Phi^{IS}(\rho,T)$ describe the way in which the system samples its ρ-dependent energy landscape as a function of T.

For simple, monatomic liquids, examination of p^{IS} and ϕ^{IS} has provided valuable insights: (1) For the single-component Lennard-Jones (LJ) fluid p^{IS} is virtually independent of T.[5] The $p^{IS}(\rho)$ relationship, on the other hand, is nonmonotonic. It displays a well-developed minimum in p^{IS} at a density ρ^*; for $\rho < \rho^*$, attractive interparticle forces are unable to sustain the system as an amorphous, isotropic, and spatially homogeneous medium. Expanding the system to lower densities fractures the inherent structures so that they consist of dense amorphous regions connected by large cavities. The point of maximum tension (minimum in $p^{IS}(\rho)$ above) is the zero-temperature limit of the superheated liquid spinodal.[4,5] (2) For a good glass-forming system, the binary LJ mixture whose parameters are chosen to represent the 80% Ni + 20% P alloy, $\phi^{IS}(T)$ is independent of T at sufficiently high T. However, when the temperature drops below a certain value T^*, ϕ^{IS} displays a marked, continuous drop upon isochoric cooling. When this happens, the activation energy for structural relaxation becomes temperature-dependent (i.e., non-Arrhenius) and the kinetics of structural relaxation becomes nonexponential.[2]

The results reported here for the SPC/E model of water show some similarities but also important differences with respect to monatomic liquids. In particular: (1) p^{IS} depends strongly on both T and ρ. The nonmonotonic $p^{IS}(\rho)$ function depends on the temperature of the equilibrated liquid from which the inherent structures are generated. (2) $\phi^{IS}(T)$ displays the same marked, continuous drop upon isochoric cooling below a characteristic T^*. This is consistent with fragile behavior at moderate supercoolings[2,18,19] (we use the term fragile in the sense advanced by Angell,[18] namely a liquid whose structural relaxation deviates from Arrhenius behavior[2]). (3) Over an extended density range, ϕ^{IS} for amorphous configurations is lower than for crystalline arrangements. Furthermore, ϕ^{IS} is very close to the limiting value corresponding to defect-free crystalline polymorphs or combinations of polymorphs. This bounds

ϕ^{IS} from below for amorphous packings, causing ϕ^{IS} at low temperature to become T-insensitive. This is consistent with a fragile-to-strong transition in water's relaxation behavior, in agreement with the scenario proposed recently by Ito et al.[19] who combined thermodynamic and kinetic measures of fragility (strong liquids, in Angell's terminology, exhibit Arrhenius behavior in the T-dependence of their characteristic relaxation times.[8,18]) (4) The density range over which SPC/E water exhibits amorphous inherent structures that are more stable than crystalline arrangements coincides with conditions at which polyamorphism between glassy phases occurs.[13,14] Thus, the energy landscape analysis suggests that polyamorphism in water occurs at densities where the liquid no longer has a ground-state that is composed of only a single crystalline polymorph and therefore experiences fluctuations toward more than one ordered arrangement.

The remainder of the paper is organized as follows. The methods used for generating equilibrium and IS configurations for SPC/E water are described in section II. Section III presents in detail the results summarized above, and these are discussed in section IV along with suggested topics for future research.

II. Methods

Constant ρ, T molecular dynamics (MD) simulations of SPC/E[15] water were used to generate configurations for the equilibrium fluid along isochores of 1.08, 1.0, 0.966, 0.94, and 0.92 g/cm³ between $T = 500$ and 230 K, with additional low-T runs for the 0.966, 0.94, and 0.92 g/cm³ isochores down to 180 K. For the two isotherms 260 and 400 K the densities simulated were from 0.8 to 1.25 g/cm³. The simulation protocol used the standard SPC/E water–water interaction potential parameters, a cubic box of 250 molecules with periodic boundary conditions, and the reaction field method for long range interactions.[20,21] A shifted force Lennard Jones(LJ) interaction[22] was used in both the simulations and generation of ISs and was chosen to taper linearly to zero between $R_t = 7.52$ Å and a cutoff distance of $R_c = 7.9$ Å. This was necessary in order for the system to be amenable to the energy minimization techniques used to generate ISs (see below). The same values of R_t and R_c were used in the reaction field treatment of long-range forces.[20] The equations of motion were integrated with a velocity-Verlet and RATTLE[22] algorithm using a time step of 0.002 ps.

The liquid was first generated from a body-centered cubic lattice scaled to the appropriate density that was then melted by simulating for 200 ps at 500 K. For each state point reported, the equilibration portion of the MD run was between 100 and 2000 ps, depending on the temperature and density, followed by an ensemble averaging period of at least twice the duration of the equilibration period. Configurations for use in generating ISs were saved from the ensemble averaging portions at intervals of between 1 and 20 ps, with the longer intervals employed at lower T. Below $T = 230$ K the root-mean-squared displacement of the molecules was not sufficient (i.e., greater than ca. 6 Å, or ca. two Lennard Jones diameters for the SPC/E potential) to ensure ergodic sampling and thus be considered representative of the equilibrated liquid. On the time scales of the simulations conducted here these are considered to be glasses, which will later be seen to be consistent with the results presented in section III.

The liquid ISs were generated by performing a conjugate-gradient numerical approximation to steepest descent energy minimization[23–25] of instantaneous MD configurations to the corresponding local potential energy minimum. This was aided by transforming the atomic coordinates for each water molecule

into the corresponding center-of-mass and Euler angle representations.[26] The transformation was necessary to maintain the rigid molecular geometry of the SPC/E potential[15] and so to be consistent with the simulated equilibrium liquid. Rigidity is maintained in the simulations via the RATTLE algorithm, which is not applicable in the conjugate-gradient method. Each minimization was considered complete when $(6N)^{-1}\sum_i (\partial \phi^*/\partial x_i)^2 < 10^{-12}$, where $\phi^* = \phi E_0^{-1}$, ϕ is the potential energy per molecule, x is either a center-of-mass coordinate scaled by the LJ radius (a = 3.1656 A) or an Euler angle, $E_0 = (q_{SPCE}e)^2/(4\pi\epsilon_0\sigma)$, e is the fundamental charge of an electron, ϵ_0 the permittivity constant, $q_{SPCE} = 0.4238^{15}$ is the partial charge on each hydrogen atom, and the i summation is over the 6N degrees of freedom ($3N$ center of mass coordinates and 3N Euler angles). For each state point,. between 20 and 50 configurations were "quenched" to their corresponding IS for calculating p^{IS} and ϕ^{IS} and for performing the structural analyses presented in section III.

The crystalline ISs were determined by taking the experimental coordinates of the oxygen atoms in a type-1 clathrate structure[28] minus its guest molecule, in ice I_h,[29] and in ice III,[29] and placing the 0 atom of an SPC/E water molecule on each of these sites. In the experimental systems the internal HOH angles of water molecules are not necessarily 109.5°, the value for the SPC/E potential. To maintain the 109.5" HOH angle it was necessary in some cases to place the H atoms in positions which do not lie exactly along the line of centers between nearest-neighbor 0 atoms. In these cases the H atoms were placed so as to maintain a 109.5" internal HOH angle while making each OH···O angle simultaneously as close to 180" as possible. Within these considerations, the H atoms were placed in such a way as to minimize deviations from H-bond linearity for every 000 triplet composed of a central H-bond donor and two acceptor molecules. This assured that all molecules were hydrogen-bonded to exactly four neighbors as in the experimental structures, with proton-ordered patterns so as to yield energies as close as possible to the ground state values. The energies per molecule of these assumed ground states were determined using exactly the same treatments of the intermolecular interactions as in the MD simulations and ϕ minimizations. Since the crystalline polymorphs were not commensurate with the cubic symmetry enforced in the MD simulations, each crystalline configuration of molecules was generated by taking a sufficient number of unit cells to provide a "core" configuration of at least 250 molecules, all of which were farther than R_c from the boundary of the overall system. To determine ϕ as a function of ρ for each of these crystalline configurations the systems were isotropically expanded or contracted from the volumes corresponding to the experimental unit cell dimensions. The ground-state energies are equivalent to the lowest possible values for ϕ^{IS} for the pure crystalline forms of the (shifted force) SPC/E model. For all structural analyses discussed in later Sections, the density used for each crystalline polymorph was that at which its ϕ^{IS} was a minimum. Finally, for purposes of structural analysis of the HB network a purely geometric HB definition was employed. Two molecules were considered to be hydrogen-bonded if their O-O distance was less than the distance of the first minimum in the IS radial distribution function (≈ 3.1 Å for all ρ, T considered here, data not shown) and if the O–H···O angle was greater than 160".

III. Results

Figure 1 shows the equilibrium pressure along isochores for the shifted-force SPC/E model used in this work. The minima
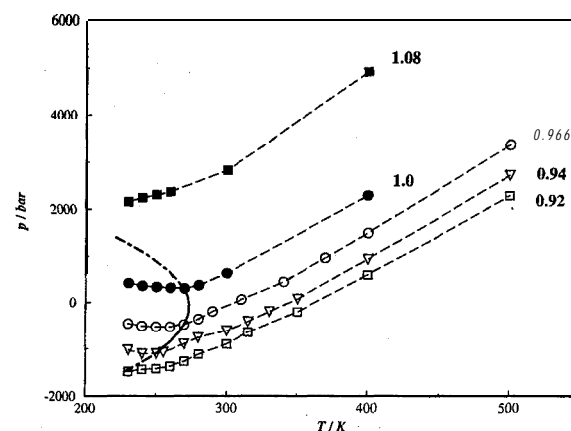

Figure 1. $p-T$ projection of isochores in the equilibrium shifted-force SPC/E liquid. The dashed curve is a guide to the eye for the locus of the minima, representing the temperatures of maximum density (TMD). The densities of the isochores are ($[=]$ g/cm³) 0.92(unfilled squares), 0.94(triangles), 0.966(unfilled circles), 1.0(filled circles), and 1.08 (filled squares). Error bars are smaller than the size of the symbols.
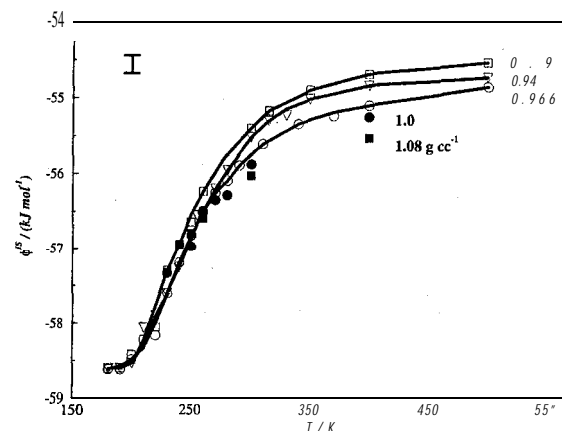

Figure 2. ϕ^{IS} as a function of liquid temperature along several isochores. The symbols for different isochores are the same as in Figure 1. A typical error bar is included in the upper left corner.

correspond to points along the locus of temperatures of maximum density (TMD). An estimate of the TMD is included as a guide to the eye. The value of the TMD at ambient pressure is ca. 274 K (vs 277 K in real water) and the retracing of the TMD occurs at ca. 275 K and -200 bar.

Figure 2 shows ϕ^{IS} as a function of T along isochores of .92 to 1.08 g/cm³. The important features shown by all five isochores are (1) a high-T plateau in which ϕ^{IS} is virtually independent of T, (2) an intermediate-T region in which ϕ^{IS} changes very rapidly with T, and (3) a *low-T* region where ϕ^{IS} shows almost no change with T. *This* form of ϕ^{IS} is very similar to that seen in an analogous study of a fragile glass-former modeled after the 80% Ni 20% P alloy,[2] in which no orientation-dependent interactions exist. The high-T behavior of ϕ^{IS} is a consequence of the liquid having sufficient thermal energy to sample the entire energy landscape available at the given p. *The* plateau is indicative of the preponderance of shallow minima relative to the deeper but rarer minima sampled at lower temperatures! Upon cooling into the intermediate-T range, the liquid becomes increasingly more biased toward low-4 basins on the landscape and encounters correspondingly higher barriers to structural transitions between basins associated with significantly different ISs. For the above-mentioned model binary alloy this transition from the high-T plateau to the intermediate-T exploration of progressively deeper basins has been shown to correspond to the onset of non-Arrhenius dynamics, indicated by the activation
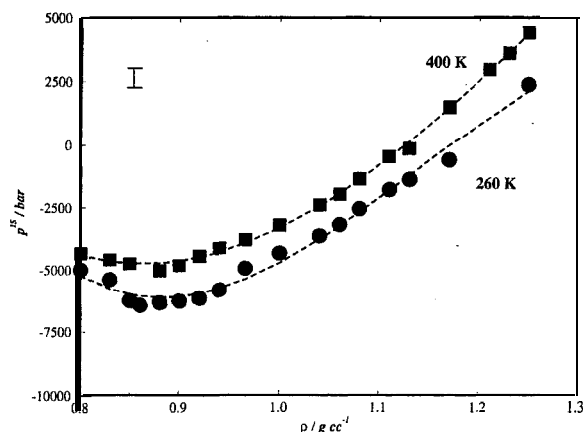
Figure 3. The equation of state of the energy landscape for the SPC/E potential: inherent structure pressure as a function of density $p^{IS}(\rho)$ along isotherms of 260 K (circles) and 400 K (squares). The temperatures are those of the equlibrated liquid from which the inherent structures were obtained. A typical error bar is included in the upper left comer.

Figure 4. Snapshot of a low-density IS (0.6 g/cm^3) showing a typical system-spanning void, in this case from the lower left comer to the upper right comer via the shared, periodic boundaries. The filled spheres represent the positions of oxygen atoms, and the line segments joining the oxygen atoms represent hydrogen bonds defined in Section II.

energy for structural relaxation becoming strongly T-dependent.[2] In the present case this behavior suggests that transitions between ISs which do not differ appreciably in energy (e.g., ones with only slightly different arrangements of HBs) are still easily accommodated, but those between significantly different ISs become increasingly difficult as T decreases. This is consistent with the progressive importance of network HB structures at low T, as opposed to isolated hydrogen-bonded structures at high T. Finally, consistent with the observations of Sastry et al.,[2] the *low-T* plateau corresponds to an effective glass transition. On the time scale of the simulation the liquid has lost the ability to sample its configuration space, and has become trapped in a small set of ISs having almost identical structures and energies. Large energy barriers (i.e., $\gg \beta^{-1}$) prevent the escape to significantly different basins due to the increasingly cooperative nature of such structural rearrangements in the low-T liquid or glass. The pronounced T-dependence of ϕ^{IS} is indicative of an exceptional "ruggedness" in the landscape. There is a wide range of amorphous basins in which the liquid can become trapped on its way to crystallization. In this sense, SPC/E water is a good glass-former and displays behavior characteristic of so-called fragile liquids.'* This term denotes substances whose configurational entropy decreases rapidly upon supercooling, giving rise to non-Arrhenius relaxation. The fragility of moderately supercooled water has recently been demonstrated by Angel1 and co-workers.[19] The parallel between Figure 2 and the behavior reported by Sastry et al. for the 80% Ni + 20% P Lennard-Jones mixture[2] is remarkable. It is indicative of the diversity of molecular interactions that can cause extreme ruggedness in the energy landscape. In the case of water, orientation-dependent interactions and the network structures to which they give rise at low T are responsible for the progressive deepening of basins sampled upon cooling. In the binary LJ case,[2] size disparity hinders crystallization, and the ruggedness reflects the 'variety of configurations to which the system has access given the energetic and geometric disparity between components.

The equation of state of the energy landscape is shown in Figure 3. The temperature on each curve is that of the liquid from which the inherent structures were generated. It can be seen that the mechanically stable arrangements exhibit. a maximum tensile strength at a particular density, which depends on the temperature of the equilibrated liquid. Below tbis density, p^{IS} increases (tension decreases) upon decompression. This
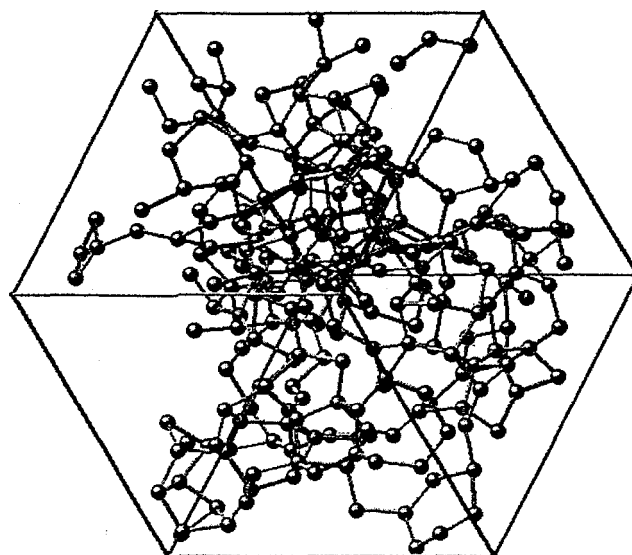
instability occurs in the absence of thermal motion, of course, and therefore is distinct from negative compressiblity states appearing' in van der Waals-type equations of state beyond the spinodal curve. The equation of state of the energy landscape of a single-component LJ system has recently been found to exhibit many of the features shown in Figure 3.[5] However, there are also important differences. Consistent with the ruggedness underlying Figure 2, the $p^{IS}(\rho)$ for SPC/E water is a function of the temperature of the equilibrated liquid. In contrast, a single curve characterizes the landscape of the single-component LJ system.[5] It is well-known that the single-component LJ system crystallizes easily in simulations,[30] and accordingly, ϕ^{IS} is expected to be virtually independent of T. Furthermore, in the LJ case the maximum tensile strength, -30 p_c (p_c being the critical point pressure), is very close to the van der Waals estimate of 27 p_c, which implies that the mechanical stability of amorphous packings and the zero-T limit of the liquid spinodal are related.[4,5] This connection is less straightforward in the present case, since the maximum tensile strength of the inherent structures is clearly T-dependent. While this tensile strength clearly increases as the T of the equilibrated liquid decreases, its relationship to a limiting tensile strength of the liquid is not obvious. In addition, it is worth noting that the minimum p^{IS} along the 400 K isotherm, ca. -5 kbar, is about 25% greater than 30 p_c for the SPC/E potential ($p_c = 139 \pm 4$ bars').'

For the single-component LJ system, Sastry et al.[5] found that at $p < \rho^*$ *the* ISs showed the onset of fissures or networks of void space, with a system-spanning cavity being observed for densities lower than ca. $0.95\rho^*$; here, ρ^* is the density at which p^{IS} is a minimum. A similar void analysis for the ISs in water was performed here as a function of p but such fissuring close to ρ^* was not observed. However, one would still expect large, system-spanning voids to form even in SPC/E water at sufficiently low density.[5,25] We found that this was indeed the case for ISs generated from the fluid at 0.60 g/cm^3 and 600 K (Figure 4).

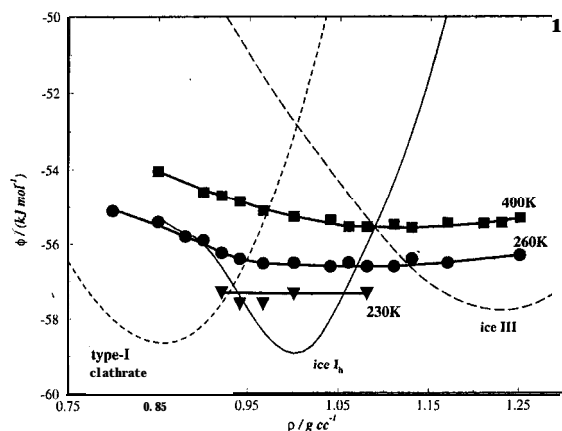An important question when considering the characteristics of the energy landscape in terms of its ISs is what are the

Figure 5. Density dependence of the inherent structure potential energy per particle, ϕ^{IS} (p) obtained from the liquid at $T = 230$ K(triangles), 260 K(circles), and 400 K(squares), along with the corresponding quantity for the ground states of the relevant crystalline structures over the density range 0.75-1.25 g/cm³. The error bars are smaller than the size of the symbols.

Figure 6. Distributions of oxygen-oxygen-oxygen angles for hydrogen-bonded molecules as a function of T and ρ in the liquid 1%: (a) as a function of T at .94 g/cm³, (b) as a function of ρ at 260 K.

absolute minima, i.e., the ordered arrays which provide the lowest potential energy as a function of density. To address this question, the energies of idealized crystalline structures for the shifted-force SPC/E model of water were calculated as a function of density. Recall from section II that these calculations are for crystalline structures taken from the experimental data at ¹one density. The energy for these configurations were calculated as the system was expanded or compressed, without allowing the configurations to relax, or equilibrate. Thus, they do not represent the inherent structures generated from a given ice polymorph allowed to equilibrate at a given density and temperature. These calculations are instead indicative of the energy of ordered structures at different densities, *if* those structures are composed solely of HB arrangements that exist in the ice polymorphs at the densities where the particular polymorph is the lowest energy structure. This point will be revisited later.

The particular polymorphs (a type-1 clathrate, ice I$_h$, and ice III) were chosen in an attempt to include the relevant experimentally known structures spanning the density range covered by the MD simulations. The superposition of the energies for the crystalline structures with the corresponding amorphous ϕ^{IS} generated from the liquid is shown in Figure 5 along different isotherms. According to the Third Law of Thermodynamics, the ground state of a macroscopic system is nondegenerate. Normally, this translates into a crystalline arrangement (He II, whose entropy at 0 K is of course zero, but which remains liquid at 0 K below 25 atm, is an exception). The energies for the individual crystalline configurations would then be expected to he below the IS energies for the liquid. What Figure 5 unambiguously shows, however, is that this reasoning is not correct for ρ values which are intermediate between ϕ (p) minima on the curves for the idealized crystalline forms. This illustrates an important point. Namely, that the "pure", or idealized, crystalline configurations are the lowest energy states only over a small range of density. For a given polymorph this would be the density range corresponding to the temperatures and pressures where it is the stable ice phase. However, Figure 5 suggests that the lowest energy states (i.e. crystalline states) for intermediate densities will either be a mixture of different crystalline polymorphs, or will have a structure which is itself intermediate between those of the polymorphs. In Figure 5 this intermediate density range is readily apparent by considering the points on the 260 and 230 K isotherms that fall below the
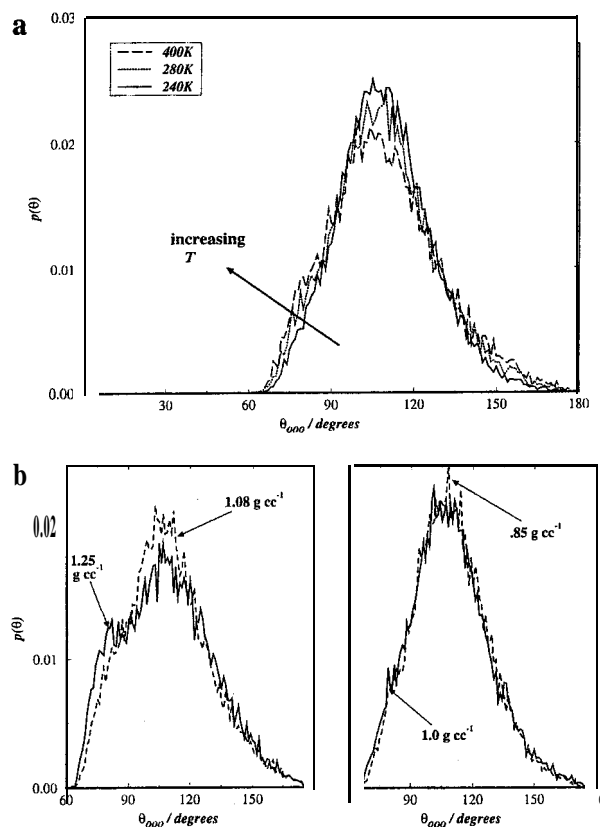
ice I and ice III ground state energies, as well as the 230 K points that fall below the type-1 clathrate and ice I curves. We interpret these data for the liquid ISs as suggesting that the lowest energy states (ground states) for these intermediate densities should contain signatures of the different polymorphic structures. Whether they are truly mixtures in the sense of polycrystalline materials, or instead that there is a uniform structure that is a hybrid of the different polymorphs is not clear, as we were not able to determine this unambiguously in tbis work. However, an investigation of the liquid ISs to help clarify the nature of the intermediate-density ground states was undertaken, and is included next.

The existence of liquid ISs with lower energies than those in idealized, "pure" structures of the crystalline polymorphs over a large range of density suggests two possible scenarios. In one, the liquid at low T samples from IS basins that are each dominated by one particular ice-like structure, with the remaining packing in a given IS being essentially noncrystalline in character. The way in which the liquid ϕ^{IS} achieves values lower than the pure polymorphs, such as seen in Figure 5, would then be by sampling a variety of ISs, each of which is reminiscent of a single polymorph. The other scenario is that the liquid samples IS basins, each of which is essentially a mixture of polymorphs, as mentioned in the preceding paragraph.

The results presented below indicate that the latter scenario is more realistic in supercooled SPC/E water. Figures 6 and 7 show this by comparing geometrical measures of the local HB network structure in the liquid ISs to those in the type-1 clathrate, ice I$_h$, and ice III structures. Similar analyses were also performed for the equilibrium liquid structures which mapped into the ISs. The only difference noted was that the calculated structural measures had larger fluctuations in the equilibrated liquid, although the mean values were not significantly different
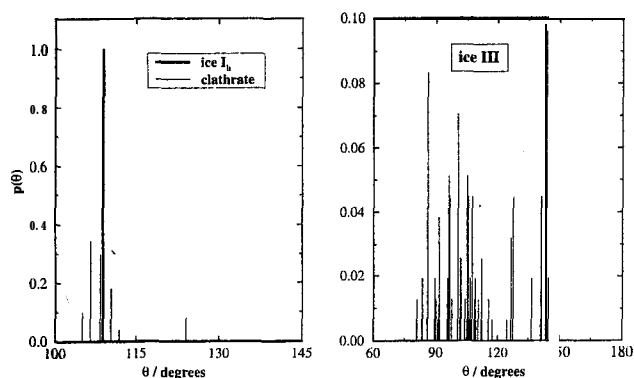
Energy Landscape of SPC/E Water

J. Phys. Chem. B, Vol. 103, No. 46, 1999 **10263**

Figure 7. Distributions analogous to those in Figure 6 for the type-1 clathrate structure at .86 g/cm^3, ice I_h at 1.0 g/cm^3, and ice III at 1.23 g/cm^3.

from the corresponding IS quantities, as expected for a liquid at low T. Note from Figure 2 that the "high" T plateau is not achieved until ca. 400 K.

Figures 6 and 7 show the distribution $p(\theta)$ of oxygen—oxygen-oxygen angles for triplets of hydrogen-bonded molecules for the liquid ISs and the different crystalline structures, respectively. Figure 6a shows this as a function of T along the 0.94 g/cm^3 isochore, and 6b shows this as a function of p along the 260 K isotherm. In all cases the liquid ISs show a strong peak at ca. $110°$, with a shoulder at ca. 90" at high T or p. Figure 7 shows that strong contributions near 110" occur for all three crystalline polymorphs, and that ice III has a comparable contribution to $p(\theta)$ at ca. 90". Since we cannot *a* priori identify features of $p(\theta)$ that are unique to each of the three crystalline polymorphs and that are obvious in the liquid ISs, we conclude that $p(\theta)$ **in the** ISs cannot be resolved unambiguously into contributions from specific types of crystalline structure (i.e., the first scenario mentioned above). Additionally, there do not appear to be any dramatic changes as a function of p or T in the "crossover" regions where the liquid ϕ^{IS} lies below the values for the individual ground-state crystalline structures (cf. Figure 5). It may be argued that the shoulder at ca. 90" that develops at high density in the liquid ISs is indicative of ice III structures, but since the same type of shoulder occurs as T increases this is instead interpreted as a mark of noncrystalline structures. Finally, the $p(\theta)$ for the liquid ISs (Figure 6) are averages over all ISs collected at a given T and p. It was also found that the $p(\theta)$ for individual ISs are virtually indistinguishable from the average over all ISs. The combination of the lack of distinguishable crystalline signatures in the liquid ISs, and the observation that $p(\theta)$ in individual ISs do not deviate significantly from the average $p(\theta)$ leads us to conclude that the latter of the two scenarios discussed above (i.e., each IS consists of multiple, distorted polymorphs) is applicable for SPC/E water. However, the conclusion that the ground state structures are a mixture of the "pure" polymorphic structures remains, as this is based on the results in Figure 5, not the analysis of the HB structures just described. The analysis of the HB network structures merely shows that the liquid samples from ISs that include combinations of different locally ordered structures. We take this as suggestive of a similar situation in the ground-state structures at the same densities since the liquid ISs at low temperature have energies which approach those expected for the ground states by linear interpolation between the ice I_h and ice III minima in Figure 5.

The above results also suggest that a comparison between larger, more cooperative HB structures may prove more fruitful
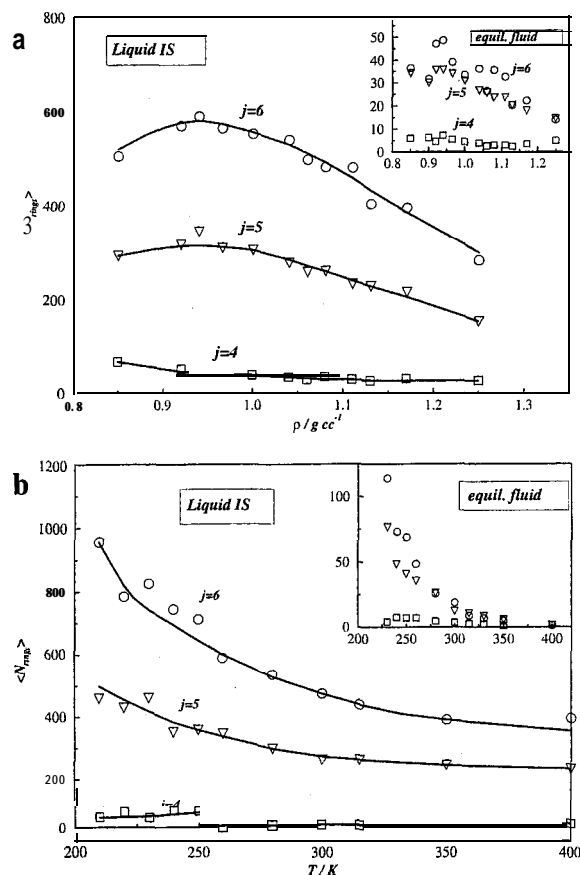

Figure 8. Average number of HB rings containing j molecules in the liquid ISs as a function of (a) ρ at 260 K, and (b) T at .94 g/cm^3. Insets are for the equilibrium liquid.

in identifying and quantifying existence or lack of ice-like structures in the liquid ISs. To this end the number of rings of HB's in the equilibrated liquid and the ISs for n -member rings (n = 4, 5, and 6) was determined as a function of p and T.

Figure 8 shows that the amounts of these ring structures are quite sensitive to T and p. Figure 8a shows the average number of n = 4, 5, and 6 rings ($N^{(4)}$, $N^{(5)}$, and $N^{(6)}$) as a function of p at 260 K in both the ISs and in the equilibrium liquid. Figure 8b shows the analogous curves as a function of T along the 0.94 g/cm^3 isochore. The amount of n = 4 rings is insensitive to p and decreases slightly with decreasing T. $N^{(6)}$ increases rapidly and monotonically with decreasing T, while as a function of p it has a maximum around 0.94 g/cm^3 at 260 K. The ratio $N^{(6)}/N^{(5)}$ stays approximately constant at 2 in both cases. The physical significance of the maxima in $N^{(6)}$ and $N^{(5)}$ as a function of p is discussed in Section IV with respect to the p^{IS} (p) minimum (Figure 3). Also included in Figures 8a and b are the values for the equilibrium fluid. It can be seen that the results are qualitatively the same, but that the absolute amounts of the rings and the scatter in the data are significantly smaller and larger, respectively, in the equilibrium configurations than in the corresponding ISs. For comparison to the crystalline polymorphs, ice III has only five-member rings, ice I has only six-member rings, and the type-1 clathrate has a mixture of five- and six-member rings with $N^{(5)}/N^{(6)} = 8$. No four-member rings are present in these crystalline polymorphs. Thus if we identify the HB rings (n = 5 and 6) as being crystalline-like, we note that their relative amounts are essentially independent of T and p but that their absolute amounts are sensitive to p, and also change rapidly within the intermediate T range where the liquid samples progressively deeper basins upon cooling (Figure 2).

10264 J. Phys. Chem. B, Vol. 103, No. 46, 1999

Roberts et al.

A further test of the differences and similarities between the HB network in the ISs and in the crystalline polymorphs was also constructed by comparing how close the rings were to being planar. To quantify the planar character of the rings a quantity S was defined as

$$s = n_{abcd}^{-1} \sum_{\langle abcd \rangle} [1 - \cos \varphi_{abcd}] \qquad (7)$$

where n_{abcd} is the number of independent torsional (0000) angles in a given polygon ($n_{abcd} = 1, 2,$ and 3 for cyclic tetramers, pentamers, and hexamers, respectively), the $\langle ... \rangle$ indicates a summation over the n_{abcd} independent angles, and φ_{abcd} is the value of a given torsional (dihedral) angle. Thus, for a completely planar geometry S = 0, and S = 2 indicates a maximum skew away from a planar geometry. However, comparison of distributions $p(S,n)$ of S for n-membered rings ($n = 4, 5,$ and 6) in the liquid ISs and crystalline ground states did not yield conclusive results. We were unable to unambiguously identify signatures of the crystalline polymorphs that were evident in the equilibrated liquid configurations or the liquid ISs, or that evolved as a function of T or ρ in these configurations or ISs. The only notable observations from this analysis are: (1) five-member rings in the liquid ISs had S = 0.01 ± 0.01 (i.e., almost perfectly planar), and (2) six-member rings in the liquid ISs had an almost uniform distribution of S between 0 and 1, which was insensitive to T and ρ; (3) $p(S,n)$ for the liquid ISs were very different from those in any of the three crystalline polymorphs considered here, indicating that any identifiable crystallites tend to experience considerable distortion.

IV. Discussion

A number of important points follow from the preceding results. First, the equation of state of SPC/E water's energy landscape, $p^{IS}(\rho)$, is strongly dependent on the temperature of the equilibrated liquid. This is in contrast to the single-component LJ case[5] where the IS equation of state is essentially independent of temperature. The observed behavior for SPC/E water reflects the biasing toward deeper basins upon lowering T. This evolution toward less strained HB structures is accompanied by an increase in tensile strength. Since the more stable HB network arrangements in water correspond to open, low-density structures,[32] the expectation is that ρ^* would decrease upon cooling. The precision of the data shown in Figure 3 does not allow this prediction to be unambiguously tested.

Second, the results for ϕ^{IS} in Figure 2 suggest that SPC/E is a fragile liquid over the T range in which the liquid equilibrated on the time scales of the MD simulations. Thus, there is a strong T-dependence of the liquid IS potential energy at moderate supercoolings, but only a weak dependence at very deep supercoolings as the liquid becomes trapped in a glassy state. However, it follows from Figure 4 that even if the liquid were to equilibrate at $T < 230$ K, ϕ^{IS} cannot continue to decrease; otherwise, amorphous structures would have lower energies than ordered ground states. Additionally, the values of the IS potential energy in the glassy states lie very close to those of crystalline ground states: compare ϕ^{IS} (190 K, 0.94 g/cm³) (Figure 2) with the lowest ϕ^{IS} values in the crystalline polymorphs (Figure 4). This suggests that the liquid immediately above its glass transition is strong,[18] while at moderate supercoolings it is fragile. Experimental evidence for this type of behavior has recently been provided by Angell and co-workers;[19] our simulations suggest a plausible molecular interpretation. The

fact that ϕ^{IS} is insensitive to ρ at low T *also* indicates that the density fluctuations which are present in an isobaric system would not alter this picture for SPC/E water.

Third, the minimum in p^{IS} in SPC/E water does not appear to correspond closely to the appearance of fissures and voids as was found in the single-component LJ fluid.[5] The maximum in $N^{(5)}$ and $N^{(6)}$ as a function of ρ in the ISs along the 260 K isotherm is suggestive of possible structural characteristics of the HB network that correlate quantitatively with the minimum in p^{IS} (p). The maximum in $N^{(6)}$ and $N^{(5)}$ at 0.94 g/cm³ and 260 K does not correspond exactly with the location of the p^{IS} minimum at $\rho^* \approx 0.87$ g/cm³ on the 260 K isotherm, indicating that the strength of HB network is not fully described only by the number of intact ring structures. A more complete structural characterization of the mechanical strength of the HB network is in progress.

Additionally, both the binary LJ system[2] and SPC/E water show strong T-dependence, below some T^*, along isochores of ϕ^{IS}. This T-dependence is attributed to the ruggedness of the energy landscape, which causes the liquid to sample progressively deeper energy basins below T^*. As mentioned above, the T-dependence of $p^{IS}(\rho)$ for SPC/E water is also attributed to the ruggedness of the landscape, and is considered to be indicative of so-called fragile glass-forming liquids. Thus, it is expected that other systems showing strong T-dependence of ϕ^{IS}, such as the binary LJ mixture investigated by Sastry et al.,[2] will also show T-dependent $p^{IS}(\rho)$. The T-dependence of the IS equation of state was not examined by Sastry et al.,[2] and so this prediction remains to be tested.

Finally, the structures underlying the liquid at low *T are highly* distorted and mixed versions of local arrangements in the crystalline polymorphs of water. There are also distinctly amorphous contributions, possibly due to the incommensurate character of the different polymorphs. This "mixture" is present in each configuration rather than resulting from a combination of significantly different configurations. It is also of interest to note that the density range over which the liquid becomes effectively "confused" as to its preferred ground state as *T* is lowered below ca. 260 K is similar to that over which the polyamorphic transition between low density and high-density amorphous ice (i.e., polyamorphism) occurs.[14] This suggests a novel, microscopic interpretation of the anomalous low-temperature phase behavior and thermodynamic properties of supercooled and glassy water in terms of its energy landscape. That is, the ground states at these intermediate densities (ca. 1.05−1.20 g/cm³) have to be combinations of the stable ice polymorphs in water. Such mixed ground states have higher energies than the ground states corresponding to the pure ice polymorphs. In addition, the liquid (or glassy) ISs have energies that are unusually close to those of the crystalline ground states. Thus at low temperature, where the free energy of condensed systems is dominated by internal energy, the liquid (or glass) may exhibit polyamorphism over a range of pressures where the system's energy can be minimzed by sampling from the ISs in the vicinity of the pure ice polymorphs, rather than from ISs which are themselves distorted mixtures of polymorphic structures. In this context, it is also worth noting that SPC/E water may be stable in crystalline arrangements that do not correspond to any polymorphs found in experiments.[33] Such structures were not included in this work, but it is of interest to include them in future work. In particular it would be interesting to see if these structures have ground-state energies that are comparable to the lowest energies calculated here for ice I_h and ice III. The existence of additional crystalline phases in different

models for water raises the interesting question of how the energy landscape differs for the various conventional models used to simulate water.

Topics currently being pursued in light of these results include the detailed characterization of the structures that confer tensile strength to the HB network (see Figure 8); investigating the particular features of different types of molecular systems that can give rise to a strong temperature dependence of $p^{IS}(\rho)$; investigating water rotational dynamics across the temperature range shown in Figure 2; and a more detailed characterization of water ISs under conditions where the ground state is expected to by polycrystalline, with the goal of better identifying signatures of crystallinity.

References and Notes

(1) Frauenfelder, H., Ed. *Landscape Paradigms in Physics and Biology. Concepts, Structures, and Dynamics;* North-Holland-Elsevier: New York, 1997.

(2) Sastry, S.; Debenedetti, P. G.; Stillinger, F. H. Nature 1998, 393, 554.

(3) Stillinger, F. H. Science 1995,267, 1935.

(4) Debenedetti, P. G.; Stillinger, F. H.; Truskett, T. M.; Roberts, C. J. *J. Phys.* Chem. *B* 1999, 103, 7390.

(5) Sastry, S.; Debenedetti, P. G.; Stillinger, F. H. Phys. *Rev. E* 1997, 56, 5533.

(6) Hare, D. E.; Sorensen, C. M. *J. Chem. Phys. 1987, 87, 4840.*

(7) Eisenberg, D.; Kauzmann, W. *The Structure and Properties of Water;* Oxford University Press: New York, 1976; pp 171-189.

(8) Debenedetti, P. G. *Metastable Liquids. Concepts and Principles;* Princeton University Press: Princeton, NJ, 1996.

(9) Stillinger, F. H.; Debenedetti, P. G. *J. Phys. Chem.* B 1999,103, 4052.

(10) Speedy, R. J.; Angell, C. A. *J. Chem.* Phys. 1976, 65, 851.

(11) Angell, C. A.; Oguni, M.; Sichina, W. *J. J. Phys.* Chem. **1982, 86,** 998.

(12) Tombari, E.; Ferrari, C.; Salvetti, G. **Chem. Phys. Lett. 1999,300, 749.**

(13) Misbima, 0.; Calvert, L. D.; Wballey, E. *Nature 1985, 314, 76.*

(14) Mishima, 0. J. Chem. Phys. 1994, 100, 8.

(15) Berendsen, H. J. C.; Grigera, J. R.; Straatsma, T. P. *J. Phys. Chem. 1987, 91, 6269.*

(16) Stillinger, F. H.; Weber, T. A. *Science* 1984,225, 983.

(17) Stillinger, F. H. *Phys. Rev. E* **1999,** *59, 48.*

(18) Angell, C. A. Science 1995,267, 1924.

(19) Ito, K.; Moyrdhan, C. T.; Angell, C. A. *Nature* 1999, 398, 492.

(20) Steinhauser, 0. *Mol.* Phys. 1982, 45, 335.

(21) Poole, P. H.; Sciortino, F.; Essmann, U.; Stanley, H. E. **Phys. Rev. E** **1993,** *48, 3799.*

(22) Allen, M. P.; Tildesley, D. J. *Computer Simulation of Liquids;* Oxford University Press: Oxford, 1987.

(23) Press: W. H.; Flannery, B. P.; Teukolsky, S. A.; Vetterling, W. T. Numerical *Recipes;* Cambridge University Press: Cambridge, 1989.

(24) Stillinger, F. H.; Weber, T. A. *J. Phys. Chem.* 1983, *87, 2833.*

(25) Corti D. S.; Debenedetti, P. G.; Sastry, S.; Stillinger, F. H. **Phys. Rev. E 1997, 55, 5522.**

(26) Goldstein, H. *Classical Mechanics,* 2nd ed.; Addison-Wesley Publishing Co.: Reading, MA, 1980.

(27) McMullan, R. K.; Jeffrey, G. A. *J. Chem. Phys.* **1965,** *42, 2725.*

(28) Franks, F. *Water: A Comprehensive Treatise;* Plenum Press: New York 1972; Vol. 1, chapter 4.

(29) Kamb, B.; Prakash, A. *Acta Crystallogr.* **1968,** *B24, 1317.*

(30) Hsu, C. S.; Rahman, A. *J.Chem. Phys. 1979, 70, 5234; J. Chem. Phys. 1979, 71,* 4974; Frenkel, D.; McTague, J. P. *Annu. Rev. Phys Chem* **1980,** *31,* 491; Cape, J. N.; Finney, J. L.; Woodcock, L. V. *J.* Chem. Phys. 1981, 75, 2366.

(31) Errington, J. R.; Panagiotopoulos, A. Z. *J. Phys. Chem.* B 1998, 102, 7470.

(32) Stillinger, F. H. Science **1980,** *209,* 451.

(33) Baez, L. A.; Clancy, P. *J. Chem. Phys. 1995, 103, 9744.*